M10e - Resonance and Phase Shift in Mechanical Oscillations

Lab Group 6: Jordan Grey([redacted])*(50%)*, [redacted]*(50%)*

December 4, 2024

Abstract

Task 1 revealed a negative linear relationship (slope = -0.77119) between ω_d^2 and δ^2, differing from the theoretical slope of -1 predicted by Eq. 3. This discrepancy is attributed to limitations in the dataset, including the trimming of higher current deflection paths lacking clear peaks and troughs, and the application of a rolling mean to reduce noise, which may have compromised data integrity. Despite these challenges, the correlation between fitted and theoretical results ($r^2 = 0.89163$) is stable but potentially misleading due to the narrow range of $x \in [0, 2.25]$.

Modeled filtered data was found to be in strong agreement with high precision and accuracy (e.g., $r^2 = 0.99916$ for the 800 mA dataset, lying within measured uncertainty. However, small variations in the datasets significantly impacted later analyses of ω_d^2 and δ^2. Future work should explore improved noise reduction methods and increase initial ϕ_0 from $\sim$ 1rad to $\sim \frac{\pi}{2}$ to enhance the number of discernible periods over the analysis duration. For Task II, the analysis of the rotary pendulum system yielded the following key parameters: damping constant $\delta = 0.005$, resonance frequency $\omega_0 = 0.231\,\text{rad/s}$, quality factor $Q = 23.1$, and resonance amplitude $A = -122.97\,\text{rad}$. The deflection angle fit was characterized by parameters $(A, \alpha, \beta, C) \to (0.083, 1.212, 0.117, -1.995)$ with $r^2 = 0.9838$, while the driving angle parameters were $(A, \alpha, \beta, C) \to (0.072, 1.211, 0.021, -1.995)$ with $r^2 = 0.9929$. Despite a fitted phase shift range of ± 0.02, values derived from angular frequencies were ten times larger, highlighting significant discrepancies due to noise and irregularities in the experimental data.

1 Introduction

The driven rotary pendulum is a powerful model for understanding forced oscillations, resonance, and damping. By analyzing the resonance curve and phase shift, one can gain insights into the system's natural dynamics, energy dissipation, and response to external forcing. This report aims to study the motion of an experimental rotary pendulum, Pohl's Wheel and determine parameters of damped harmonic motion and superimposed free system and driven oscillations through a variety of methods. The experimental analysis of the rotary pendulum revealed significant challenges due to noise and irregularities in the deflected oscillation.

2 Theoretical Basis

2.1 Rotary Pendulum without External Drive

Without an External Drive the rotary pendulum, with a start position at some angle ϕ_0 from its rest position, undergoes oscillation and experiences a damping force attributable to the magnitude of the eddy currents induced in the copper disk of the rotary pendulum. This results in the homogeneous equation of motion [1]:

$$\ddot{\phi} + 2\delta\dot{\phi} + \omega_0^2\phi = 0 \tag{1}$$

Where:

$$\delta = \text{Damping constant (rad/s)}$$
$$\omega_0 = \text{Angular undamped frequency (rads/s)}$$

This equation of motion gives rise to three distinct cases:

$$\begin{aligned}\text{Strong Damping} &: \delta^2 > \omega_0^2 \\ \text{Critical Damping} &: \delta^2 = \omega_0^2 \\ \text{Weak Damping} &: \delta^2 < \omega_0^2\end{aligned}$$

For the purpose of this report the case for weak damping was explored and as such the solution to Eq. 1 is given by [1]:

$$\phi(t) = Ce^{-\delta t}\cos\left(\omega_d t - \alpha\right) \tag{2}$$

Where:

$$\begin{aligned}C &= \text{Amplitude constant} \\ \omega_d &= \text{Angular damped frequency (rad/s)} \\ \alpha &= \text{Phase shift (rad)}\end{aligned}$$

It is also of note that:

$$\omega_d = \sqrt{\omega_0^2 - \delta^2} \tag{3}$$

It is important to note that ω_0 describes the angular frequency of an undamped rotary pendulum and is a property of harmonic oscillators that undergo harmonic motion. The value of ω_0 determined by the geometry and physical characteristics of the rotary pendulum and remains constant throughout the motion of the rotary pendulum. Similarily ω_d also remains constant throughout the motion of the rotary pendulum however describes the angular frequency of the rotary pendulum under damping conditions, as such the value of ω_d is a determined by the physical characteristics of the rotary pendulum and the degree of damping, δ applied on the oscillating system.

2.2 Rotary Pendulum with External Drive

A rotary pendulum driven by an external torque $M_0\sin(\omega t)$, which varies periodically in time, demonstrates an important physical phenomenon: forced oscillations. In such systems, after a transient period, the pendulum oscillates at the same angular frequency ω as the external drive, regardless of its natural frequency. This behavior is a direct result of the external periodic driving force overcoming the natural tendencies of the system, leading to steady-state oscillations with a distinct phase relationship to the driving torque. The dynamics of this system are governed by a combination of the system's natural properties (like inertia and damping) and the properties of the external drive.

The motion of the driven pendulum is described by the following second-order, linear, inhomogeneous differential equation [1]:

$$J\ddot{\phi} + \gamma\dot{\phi} + D\phi = M_0\sin(\omega t) \tag{4}$$

Where:

$$\begin{aligned}J &= \text{Moment of inertia of the pendulum } (\text{kg}\cdot\text{m}^2) \\ D &= \text{Restoring torque constant } (\text{N}\cdot\text{m/rad}) \\ \gamma &= \text{Damping coefficient } (\text{N}\cdot\text{m}\cdot\text{s}) \\ M_0 &= \text{Amplitude of the driving torque } (\text{N}\cdot\text{m}) \\ \omega &= \text{Angular frequency of the external drive (rad/s)} \\ \phi &= \text{Angular displacement of the pendulum (rad).}\end{aligned}$$

This equation is inhomogeneous due to the external driving torque term. The solution to this equation has two components:

$$\phi(t) = \phi_h(t) + \phi_p(t), \tag{5}$$

Where:

$\phi_h(t)$ = Solution to the homogeneous equation, describing the natural oscillations of the system.
$\phi_p(t)$ = Particular solution, accounting for the forced oscillations due to the external torque.

To find the steady-state oscillations of the pendulum, we assume a solution of the form:

$$\phi_p(t) = A(\omega)\sin(\omega t + \theta), \tag{6}$$

Where:

$A(\omega)$ = Frequency-dependent amplitude of oscillation.
θ = Phase shift between the driving torque and the pendulum's response.

Substituting this ansatz into the equation of motion, we obtain [1]:

$$A(\omega) = \frac{M_0}{J\sqrt{(\omega_0^2 - \omega^2)^2 + (2\delta\omega)^2}}. \tag{7}$$

This expression shows how the amplitude depends on the driving frequency ω. When the driving frequency ω is close to the natural frequency of the system, the amplitude becomes large, indicating resonance.

The phase shift θ is given by:

$$\theta(\omega) = \tan^{-1}\left[-\frac{2\omega\delta}{(\omega_0^2 - \omega^2)}\right]. \tag{8}$$

The negative sign indicates that the pendulum response lags behind the driving torque.

The general solution of Eq. 4 is :

$$\phi(t) = A(\omega)sin(\omega t + \theta) + Ce^{-\delta t}cos(\omega_d t - \alpha) \tag{9}$$

Where:

$\omega_d = \sqrt{\omega_0^2 - \delta^2}$ = Angular frequency of the damped oscillation.
C, α = Constants that match system's initial conditions.

Resonance is a phenomenon that occurs in driven oscillatory systems when the driving frequency ω approaches the system's natural angular frequency ω_0. At resonance, the amplitude of oscillation reaches its maximum, as the energy input from the external drive aligns with the natural oscillatory behavior of the system. The sharper the resonance curve and the higher the quality factor, the closer the system is to being lossless, highlighting the interplay between energy storage and dissipation. The amplitude $A(\omega)$ reaches its maximum at the resonance angular frequency ω_R, where the driving frequency matches the effective natural frequency of the system. The resonance angular frequency is:

$$\omega_R = \sqrt{\omega_0^2 - 2\delta^2}\ , \text{ for } \delta < \frac{\omega_0}{\sqrt{2}} \tag{10}$$

Where:

$\omega_0 = \sqrt{D/J},$ = Natural angular frequency of the undamped system.
$\delta = \gamma/2J,$ = Damping constant.

For weak damping ($\delta \ll \omega_0$), the resonance frequency closely approximates the natural frequency:

$$\omega_R \approx \omega_0 \approx \sqrt{\frac{D}{J}} \tag{11}$$

At resonance, the amplitude is maximized:

$$A(\omega_R) = \frac{M_0}{\gamma\omega_d} \text{ , for } \delta < \frac{\omega_0}{\sqrt{2}}.$$
$$A(\omega_R) = \frac{M_0}{D} \text{ , for } \delta > \frac{\omega_0}{\sqrt{2}}.$$

The resonance curve is a plot of $A(\omega)$ versus ω, showing how the amplitude of oscillations changes with the driving frequency. The curve is sharply peaked at ω_R, with its sharpness determined by the damping. The half-width $\Delta\omega$ of the resonance curve is the difference in frequencies at which the amplitude drops to $A(\omega_R)/\sqrt{2}$ [1]:

$$\Delta\omega = 2\delta. \tag{12}$$

The phase shift $\theta(\omega)$ varies smoothly from 0 to $-\pi$ as ω increases. This reflects the gradual transition from in-phase motion (low ω) to out-of-phase motion (high ω). At natural frequency ω_0, the phase shift has an inflection point, indicating a critical change in the behavior of the system.

The quality factor Q is a measure of how sharply the system resonates [1]:

$$Q = \frac{\omega_0}{2\delta}. \tag{13}$$

A higher Q value corresponds to lower damping, meaning sharper resonance and longer-lasting oscillations.

3 Tasks

3.1 Task I

3.1.1 Experimental Setup

To determine the angular damped frequency ω_d across a range of differing a damping constants, The pairs of coils on a Pohl's Torsion Pendulum was connected to a DC power supply with a variable current I. Also attached to the Pohl's Torsion Pendulum is a ferromagnetic needle and digital angle sensor to measure the deflection angle of the pendulum over time.

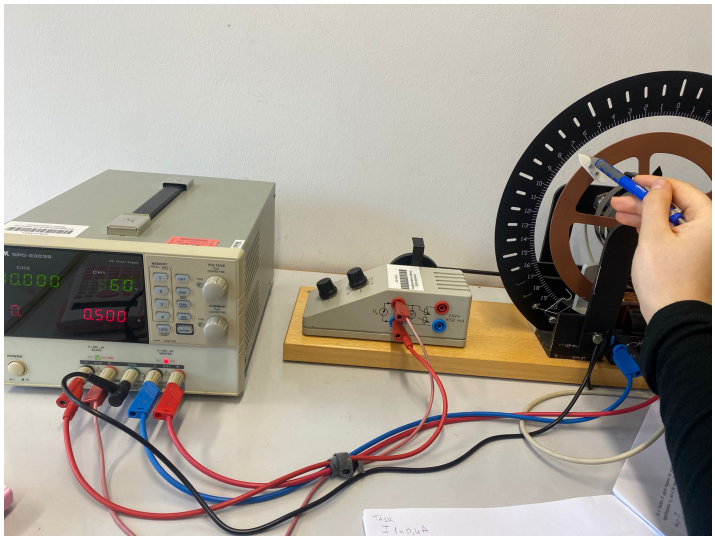

Figure 1: Task1 Experimental Setup

With initial deflection angle of $1rad$, the deflection angle was recorded for a span of at least $10s$, over the current range of $400mA$ to $1200mA$ in $80mA$ intervals to record the affect damping constant δ has on the motion of the rotary pendulum. Through use of Eq. 2 A model was then constructed with the measured results to determine both δ and ω_d. These determine values for each set of data was then used to plot ω_d^2 against ω_0^2 and was compared with the theoretical relationship of Eq. 3

3.1.2 Data Analysis

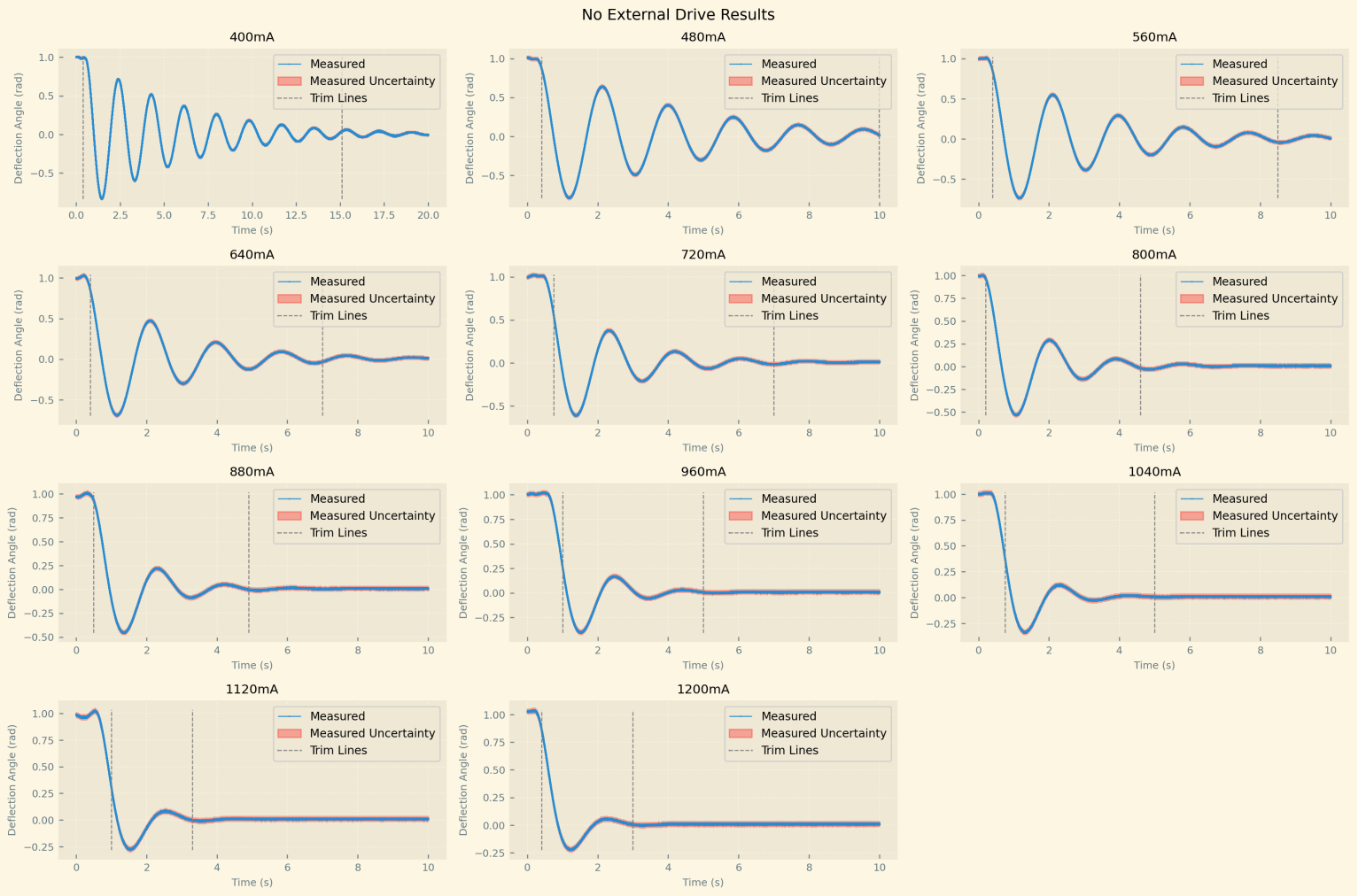

Figure 2: Recorded Data for all Currents

Fig. 2 shows the raw data collected along with its uncertainty, it can clearly be seen that as the current increases the damping constant increases. It is also of note that the measured uncertainty of the deflection angle is comparatively small. The trim lines indicate the focus area of each dataset that was used for further analysis as outside this area there is noise from releasing the pendulum, *(at the beginning of the dataset)*, or the peaks and troughs becomes difficult to model with the uncertainty and high frequency noise of the measured results, *(towards the end of the dataset)*.

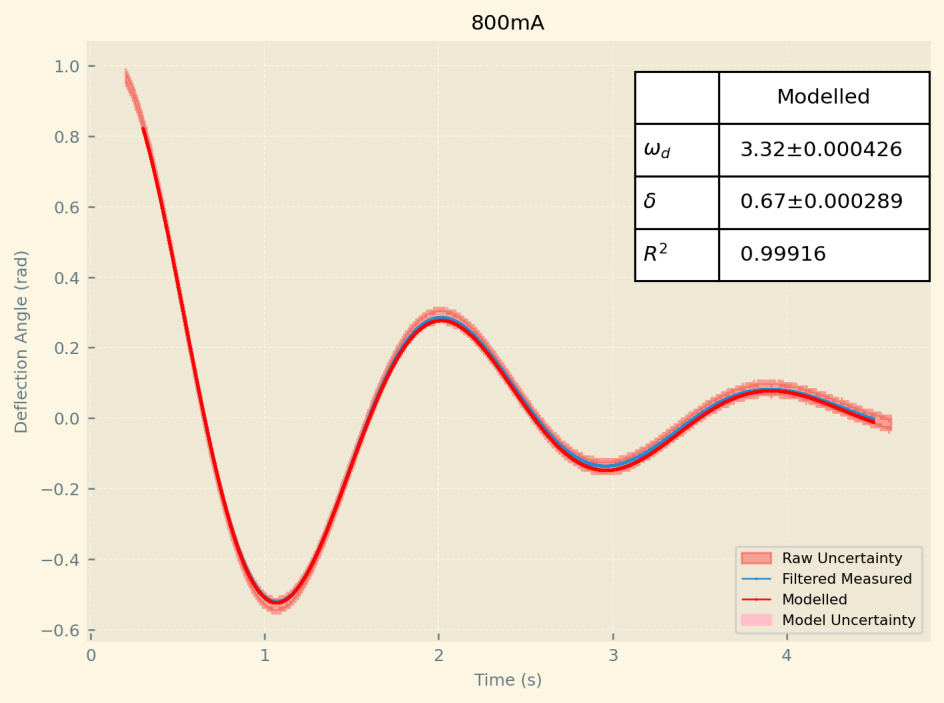

Figure 3: Filtered and Modeled Deflection Angle for $I = 800$mA

To better model the data to Eq. 2 a rolling mean with window size 1000 was applied to the data to filter out the noise, then each dataset was modeled and values for ω_d and δ determined, along with a r^2 value to determine the correlation between the filtered data and the model. Fig. 3 shows the dataset for 800mA through the pair of coils. Both the filtered Measured data and the modeled trajectories of the deflection angle remain inside the uncertainty of the measured data. The graph also show the uncertainty of the modeled however this is quite small as it was determined from the uncertainty in filtered data along with the uncertainties that arose from the determining ω_d and δ. The strong correlation between the filtered data and the modeled of $r^2 = 0.99916$ along with both of these lines being inside the raw uncertainty for 800mA suggest both accuracy and precision. This level of precision is present for all of the amperages used and can be viewed in the Appendix.

I **(mA)**	δ**(rad/s)**	ω_d**(rad/s)**
400	$0.185 \pm 5.97 \times 10^{-5}$	3.37 ± 0.000257
480	$0.257 \pm 9.58 \times 10^{-5}$	3.37 ± 0.000313
560	0.346 ± 0.000147	3.37 ± 0.000394
640	0.438 ± 0.000183	3.35 ± 0.000433
720	0.551 ± 0.000271	3.34 ± 0.000737
800	0.670 ± 0.000289	3.32 ± 0.000426
880	0.805 ± 0.000412	3.30 ± 0.000412
960	0.935 ± 0.00083	3.27 ± 0.00258
1040	1.09 ± 0.00117	3.23 ± 0.00266
1120	1.19 ± 0.00118	3.18 ± 0.00369
1200	1.50 ± 0.00104	3.13 ± 0.0017

Table 1: ω_d vs. δ for each current I

Table. 1 Shows δ and wd for each amperage it is apparent that as the current through the pair of coils increases, the damping constant increases however this relation is not strictly linear. There is little to be drawn from the relationship between the angular damping constant and the damping constant from Table1. The uncertainty in every value is almost insignificant suggesting a high degree of precision in the data determined.

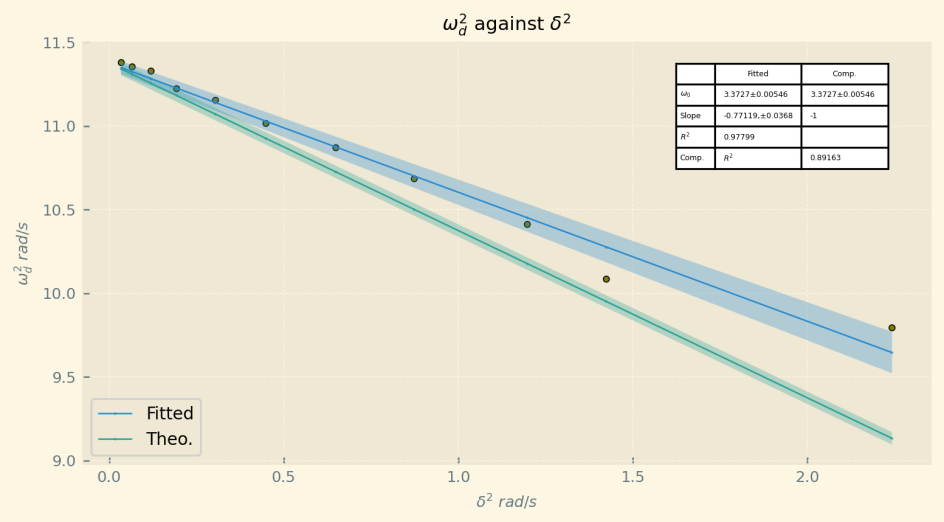

Figure 4: Plotted ω_d^2 against δ^2

Fig. 4 plots the square of the values from Table. 1 along with a fitted line of best fit and the theoretical relationship between ω_d^2 and δ^2. It is clear that the results of Table 1 have a slope $= -0.77119$ which differs significantly from the theoretical slope $= -1$. Here both the fitted and the theoretical were provided with an intercept value of ω_0^2 determined from experimental methods as the theoretical value of ω_0^2 was not known. The uncertainty in the theoretical is a result of the uncertainty in ω_0^2, whereas the fitted uncertainty arises from both uncertainty in ω_0^2 and uncertainty in the modeled slope. The fitted line of best fit has an $r^2 = 0.97799$ with experimental data points and a compared $r^2 = 0.89163$ with the theoretical line. This is unexpectedly high considering the differences in slope however this is attributable to the limited range of $x \in [0, 2.25]$.

3.2 Task II

Measure the resonance curve of a rotary pendulum as well as the phase shift between drive and deflection of the pendulum disc for one value of the damping constant. Plot the resonance curve, compare with theory by making a nonlinear fit and determine resonance frequency and damping constant. Plot the phase shift and compare with theory by making a nonlinear fit. Determine the phase shift θ by measuring the time delay Δt between the driving torque and the pendulum's response: $\theta = \omega \Delta t$.

3.2.1 Experimental Setup

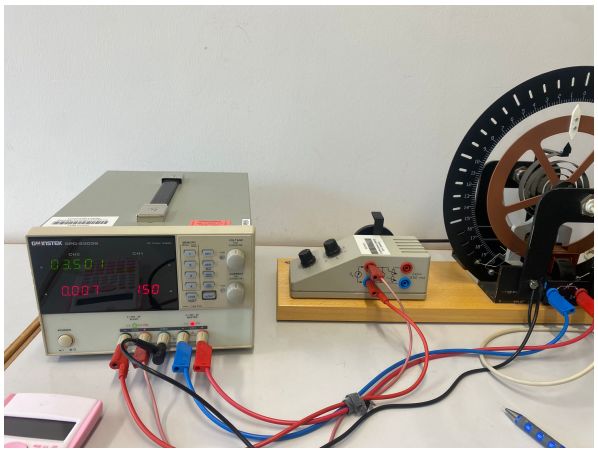

Figure 5: Experimental Setup

From the previous setup, this experiment uses a Pohl's Torsion Pendulum with an additional eddy current brake. On the channel one of the DC power supply, the voltage shows the voltage powering the Eddy brake, and, on channel two, there's a motor, providing a driving torque. For the channel two, the voltage varies across time, creating an driven oscillation. To simplify the analysis, only the data corresponding to a driving voltage of 3.5V is considered in this report.
For the resulting deflection angle of the pendulum, the voltages are related with their corresponding angles, driving and damping, by $1V \approx 90\,\text{deg} \approx 1.57$ radians.

3.2.2 Data Analysis

3.2.3 Method

For the resulting deflection angle of the pendulum, the voltages are related with their corresponding angles, driving and damping, by $1V \approx 90\,\text{deg} \approx 1.57$ radians. The values are affected by significant noise due to the number of points chosen, making the calculation of angular velocity as the derivative of the deflection angle with respect to time unreliable.Instead, the deflection angle is modeled as a function, and a best-fit curve is applied to the data to obtain a smoother and more accurate representation for further computations. Separated deflection angles can be easily expressed as sinusoidal functions. However, the resulting function obtained by isolating the driven oscillation from the damping oscillation No other fits, such as exponential or polynomial, are appropriate for the function described. The sinusoidal model used to represent the deflection angle is $y(t) = A\sin(\alpha t + \beta) + C$, where $A[rad]$, $\alpha[1/s]$, β, and $C[rad]$ are constants that are determined through curve fitting. The parameters (A[rad], α [1/s], β, C) are extracted by fitting the model to the measured deflection data. This approach is more suitable because the system's oscillatory nature is best captured by a sinusoidal function, while other forms (such as exponential or polynomial fits) would not appropriately describe the periodic behavior observed in the system. Following Eq. 9, parameters that describe the system are found using curve fit, $(M_0[rad], J[kg \cdot m^2], \omega 0[rad/s], \delta[1/s], \phi, C[rad], \alpha)$.

For the phase shift between the driven and deflected oscillation, the angular frequencies were obtained from the sum of the best fit functions. This approach was necessary because the experimental

values were too noisy for the Δt (time difference) to be reliably calculated. Additionally, the deflected oscillation was too irregular and lacked sufficient periodicity to yield a stable period for the best fit. The same logic applies to the phase shift fit, where the phase is integrated into the experimental values. The oscillation from the best-fit functions were used to model the phase shift between the driven and deflected oscillation, caused by the noise in the experimental data and the irregular periodicity of the deflected oscillation.

3.2.4 Results

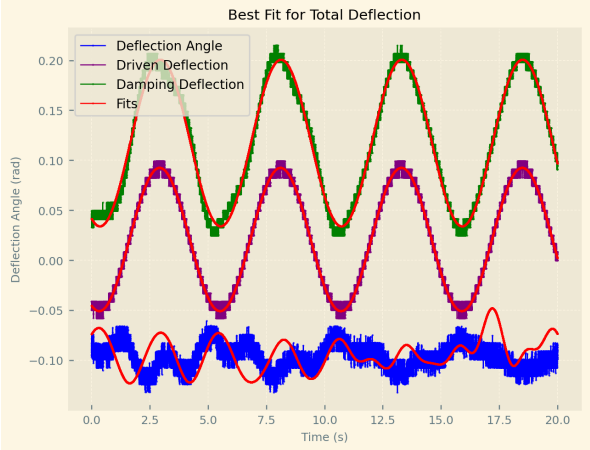

Figure 6: Total Deflection Angle

Fig.7 presents the resonance curve, which ideally should show a pronounced peak around the natural frequency ω_0, corresponding to the maximum amplitude response of the system. However, the graph appears more like a straight line because the amplitude does not reach the expected value of $\frac{1}{\sqrt{2}}$ of the maximum amplitude, which is the standard criterion for defining the resonance peak.

The data for the driving angle is characterized by the parameters $(A, \alpha, \beta, C) \rightarrow (0.072, 1.211, 0.021, -1.995)$, with $r^2 = 0.9929$. The damping angle is characterized by $(0.083, 1.212, 0.117, -1.995)$, with $r^2 = 0.9838$.

The best fit of the resulting angle has parameters $(M_0, J, \omega_0, \delta, \phi, C, \alpha) \rightarrow (-0.001, 0.132, 0.231, 0.005, -1.43, 4.6, 0.036)$, with $r^2 = -1.71$, and a quality factor of $Q = 23.1$. Using these parameters, the resonance amplitude is calculated to be $-122.97\,\text{rad}$.

Similarly, for the phase shift, Fig.9 shows the phase shift with respect to the frequency ratio.

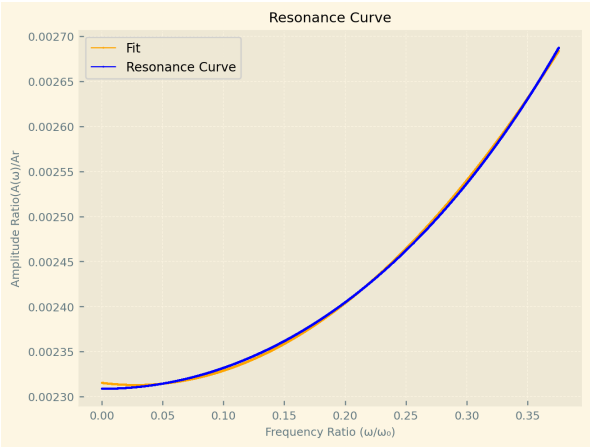

Figure 7: Resonance Curve

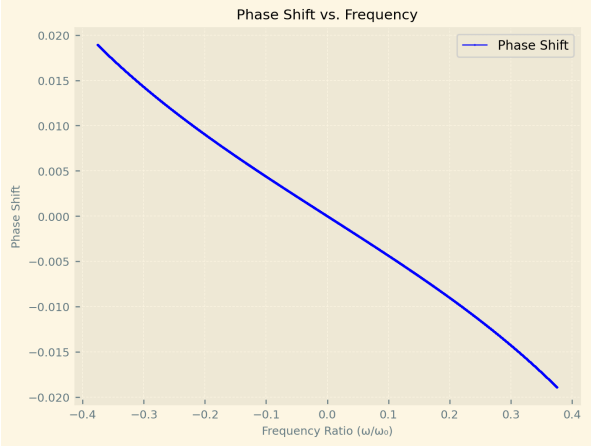

Figure 8: Resonance Curve

For a time shift $\Delta t = 2.79\,\mathrm{s}$ between the driven and deflected frequencies, Fig.9 shows the phase shift $\theta = \Delta t \cdot \omega$. The values range between $\approx \pm 0.2$.

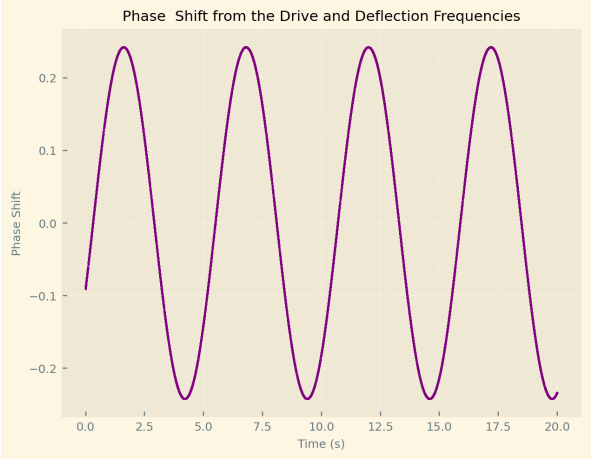

Figure 9: Phaseshift from the Driven and Deflection Frequencies

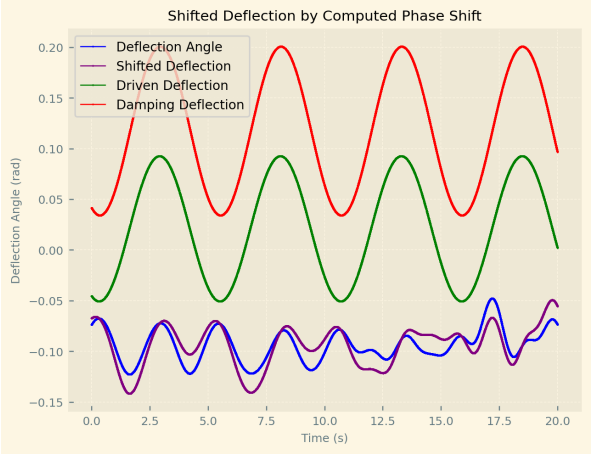

Figure 10: Fitted Phaseshift in Experimental Data

The phase shift is computed using Eq. 8, along with the system parameters determined previously,

and is plotted alongside the experimental values in Fig. 10. The fitted phase shift varies within a narrow range of ± 0.02, being visible on the graph. The value from the angular frequencies is 10 times bigger with shows a big discrepancy between the two ways of computation.

4 Discussion

4.1 Task 1

The results from the Task 1 found a negative linear relationship with slope $= -0.77119$ between the ω_d^2 and δ^2 ,(Fig. 4). This relationship differs significantly from the theoretical result determined by Eq. 3 of a negative linear relationship of slope $= -1$. It is predicted that this discrepancy is a result of; The lack of discernible peaks and troughs for the higher current deflection paths that thus required trimming to model the data and reduced the total dataset that the model was fitted to, reducing model accuracy, Fig. 2. As well as the use of a rolling mean to reduce the noise in the data to be able to model the data with use of Eq. 2., as without such a reduction, modeling each dataset proved to be quite difficult. It is predicted that more appropriate noise reduction methods exist that reduce noise in a manner that has less of an impact on data integrity.

The correlation between the fitted and theoretical relationship in Fig 4 was a stable $r^2 = 0.89163$ however this is misleading as the range of x is a narrow $x \in [0, 2.25]$.

The modeling of the filtered data onto Eq. 2 proved to be very successful with all models strong agreeing with the filtered data, Fig. 3 (and Appendix), with the 800mA dataset having $r^2 = 0.99916$ and falling within the measured uncertainty suggesting a high precision and accuracy. However as mentioned previously it is predicted that although for each current I dataset there was strong agreement, high accuracy and high precision that small variation that did arise wildly changed the relationship between the ω_d^2 and δ^2 later on in analysis. For future investigation it is suggested to increase the initial ϕ_0 from $1rad$ to $\frac{\pi}{2}$ in an effort to increase the total number of discernible periods over the span of $10s$.

4.2 Task II

Firstly, it is necessary to highlight that the experimental values suffer from significant noise and irregularities in the deflected oscillation, which undermine the reliability of the analysis. The noise in the data makes it challenging to determine accurate parameters through curve fitting, as the best-fit functions deviate from the actual physical behavior of the system. This introduces substantial errors in the derived parameters, such as the damping constant δ, the resonance frequency ω_0, and the phase shift.

Moreover, the curve-fitting process itself is affected by the quality of the data. Poor choice of sample rate, large uncertainties, and the lack of periodicity in the deflected oscillation further contribute to the inaccuracies. As a result, the computed phase shift using Eq. 8 does not match the experimental values, indicating that the model fails to capture the experimental behavior accurately under the current conditions. These issues emphasize the need for higher-quality data, improved experimental setups. Careful preprocessing methods were applied to minimize noise and filter outliers in the data. However, due to the overwhelming number of values and inconsistencies in the dataset, the code struggles to identify a clear pattern for analysis. This ambiguity further complicates the curve-fitting process and undermines the reliability of the derived parameters.

Although the dataset presents significant noise and inconsistencies, a general analysis of the overall trend can still be conducted. Despite the challenges in accurately extracting specific parameters, the broader behavior of the system provides valuable insights into its dynamics.

The resonance curve is graphed in Fig.7. The resonance curve ideally should show a pronounced peak around the natural frequency ω_0, corresponding to the maximum amplitude response of the system. However, in this case, the graph appears more like a straight line, rather than a typical resonance curve. This is because the amplitude does not grow significantly enough to reach the

expected value of $\frac{1}{\sqrt{2}}$ of the maximum amplitude (which is the standard criterion for defining the resonance peak).

In a typical resonance curve, the system's amplitude increases as the driving frequency approaches ω_0, and the amplitude reaches its maximum at this frequency. However, because the amplitude does not increase enough, the graph does not curve as it should at the resonance point. The resonance peak is expected to be sharp, and the amplitude should eventually decrease once it exceeds resonance, but here the response is too weak, and thus the curve appears more like the beginning of the resonance curve, without the full, characteristic peak.

The high correlation coefficient $r^2 = 0.99$ suggests that the data is well-represented by a function close to a cosine function. The phase shift curve should also exhibit a sharp change around resonance, where the phase shift moves from $0°$ to $90°$ (or $\pi/2$ radians), but due to the weak amplitude response and lack of a clear resonance peak, the phase shift curve behaves similarly, not showing the expected sharp transition.

The fitted phase shift varies within a narrow range of ± 0.02. However, the value derived from the angular frequencies is approximately ten times larger, underscoring a substantial discrepancy between the two methods. This discrepancy could stem from several factors, including limitations in the experimental setup, inaccuracies in the measured angular frequencies, or deviations in the system's behavior from the assumptions made in the theoretical model.

The experimental phase shift may also be influenced by noise and irregularities in the deflected oscillation, leading to errors in the calculated values. Additionally, the fitted phase shift, based on the best-fit function, may oversimplify the system's dynamics and fail to capture complex interactions affecting the oscillation. These inconsistencies suggest a need for refined experimental techniques, improved parameter estimation, and further investigation to reconcile the observed differences.

For future investigations, in addition to minimizing noise in the graphs and decreasing the sample rate, a greater voltage is necessary to provide data that more smoothly represents the resonance phenomenon and better aligns with the theoretical model. Furthermore, improvements in data acquisition techniques and experimental setup could enhance the accuracy and reliability of the results.

References

[1] M. Ziese. *M10e Resonance and Phase Shift in Mechanical Oscillations.* Universität Leipzig, December 2024.

5 Appendix

Figure 11: Filtered Data for all Currents